

# What is the Entanglement Length in a Polymer Melt?

Mathias Pütz <sup>\*×</sup>, Kurt Kremer <sup>\*+</sup> and Gary S. Grest <sup>+</sup>

<sup>\*</sup> Max-Planck-Institut für Polymerforschung, Postfach 3148, D-55021 Mainz, Germany

<sup>+</sup> Sandia National Laboratories, Albuquerque, NM 87185-1411, USA

<sup>×</sup> present address: Sandia National Laboratories, Albuquerque, NM 87185-1349, USA

We present the results of molecular dynamics simulations of very long model polymer chains analyzed by various experimentally relevant techniques. The segment motion of the chains is found to be in very good agreement with the reptation model. We also calculated the plateau modulus  $G_N^0$ . The predictions of the entanglement length  $N_e$  from  $G_N^0$  and from the mean square displacement of the chain segments disagree by a factor of about 2.2(2), indicating an error in the prefactor in the standard formula for  $G_N^0$ . We show that recent neutron spin echo measurements were carried out for chain lengths which are too small to allow for a correct determination of  $N_e$ .

How an entangled polymer chain moves in a dense melt of other chains has been a long standing problem. The most widely accepted picture is that the chains reptate like a snake [1,2]. For short times chains move isotropically until they feel the constraints of their neighboring chains. For intermediate times, the chain segments move along the path or tube created by the surrounding chains in a Rouse-like [3] motion. Only the ends explore new space. For the inner section of the chain, this Rouse-like motion on a contour which is also a random walk gives rise to the famous  $t^{1/4}$  power law regime in the mean-square displacement of the beads  $g_1(t)$ . For very long time, the motion is diffusive, with a chain diffusion constant  $D$  that scales as  $N^{-2}$  for large  $N$ , where  $N$  is the chain length. For short chains, the motion is much simpler and can be approximately described by the Rouse model and  $D \sim N^{-1}$ . To characterize the crossover between the Rouse and reptation regime, one can define an entanglement length  $N_e$ . Within the reptation model,  $N_e$  can be related to both the tube diameter  $d_T$  and crossover time  $\tau_e$  from the early time Rouse regime where  $g_1(t) \sim t^{1/2}$  to the  $t^{1/4}$  regime as well as from the value of the plateau modulus  $G_N^0$ . Over the years there have been a number of experiments [4–6] and simulations [7–11] designed to test various aspects of the theory. Recent neutron spin echo (NSE) scattering experiments [6] which measure the dynamic structure factor  $S(k, t)$ , suggest that  $N_e$  as measured from  $d_T$  is consistent with that determined from  $G_N^0$ . Our previous simulation results [7,9] suggested an inconsistency in that  $N_e$  measured from  $g_1(t)$  was about one half that measured from  $S(k, t)$ , though both  $g_1(t)$  and  $S(k, t)$  are single chain quantities and measure the same motion. However since the chains were only a few  $N_e$  ( $N \leq 200$ ), our results were not conclusive. We have now extended our simulations to much longer chains, as long as  $N = 10000$ , and measured not only single chain quantities but also  $G_N^0$ . We find clear evidence for differences on the order two between  $N_e$  measured from  $g_1(t)$  or  $S(k, t)$  and that from  $G_N^0$ . The previous reported agreement in  $N_e$  determined from NSE data for  $S(k, t)$  and  $G_N^0$  is shown to be largely due to finite chain length effects in  $d_T$  as determined from  $S(k, t)$ .

To overcome the long time scales needed to simulate a melt of long entangled polymers, we use a coarse grained model

in which the polymer is treated as a string of beads of mass  $m$  connected by a spring. The beads interact with pure repulsive Lennard-Jones excluded volume interactions (cutoff at  $2^{1/6}\sigma$ ) and are connected by a finite extensible non-linear elastic potential (FENE) between neighbors along the chain (see e.g. [7] for details). The model parameters are the same as in ref. [7]. The temperature  $T = \epsilon/k_B$ , where  $\epsilon$  is the strength of the Lennard-Jones interaction. We use dimensionless units in which  $\sigma = 1$  and  $\epsilon = 1$  and the basic unit of time  $\tau = \sigma(m/\epsilon)^{1/2}$ .

We performed constant volume simulations of monodisperse polymer melts at a segment density of  $\rho = 0.85\sigma^{-3}$ . The temperature was kept constant by coupling the motion of the beads weakly to a heat bath with a local friction coefficient  $\Gamma = 0.5\tau^{-1}$ . The equations of motion were integrated using a velocity Verlet algorithm with a time step  $\Delta t = 0.012\tau$ . The average bond distance is  $\sqrt{\langle l^2 \rangle} = 0.97\sigma$  and chain stiffness  $c_\infty = 1.75$ . This gives a statistical segment length of  $b = 1.28\sigma$ . Initial conformations of the chains were grown as non-reversal random walks with the proper melt end-to-end extension. Resulting initial overlaps of chain segments were removed by simulating a soft core potential for a very short time to avoid instabilities with the Lennard-Jones potential. Initially [7], we studied chains of length  $5 \leq N \leq 200$  and later reran [9] all the systems for  $N \leq 200$  with more chains for longer times to improve the quality of the data. Our new results are for a system of  $M$  chains of length  $N$ , for  $M/N = 120/350, 350/700$  and  $50/10000$ .

The most direct route to verify the predictions of the reptation model is to monitor the mean-square displacements of the segments  $\mathbf{r}_i$ ,

$$g_{i,1}(t) = \left\langle (\mathbf{r}_i(t) - \mathbf{r}_i(0))^2 \right\rangle \quad (1)$$

$$g_{i,2}(t) = \left\langle (\mathbf{r}_i(t) - \mathbf{r}_{cm}(t) - \mathbf{r}_i(0) + \mathbf{r}_{cm}(0))^2 \right\rangle, \quad (2)$$

and the center of mass of the chains  $\mathbf{r}_{cm}(t)$ ,

$$g_3(t) = \left\langle (\mathbf{r}_{cm}(t) - \mathbf{r}_{cm}(0))^2 \right\rangle. \quad (3)$$

The reptation model predicts the following power laws for various time regimes [1,2]:

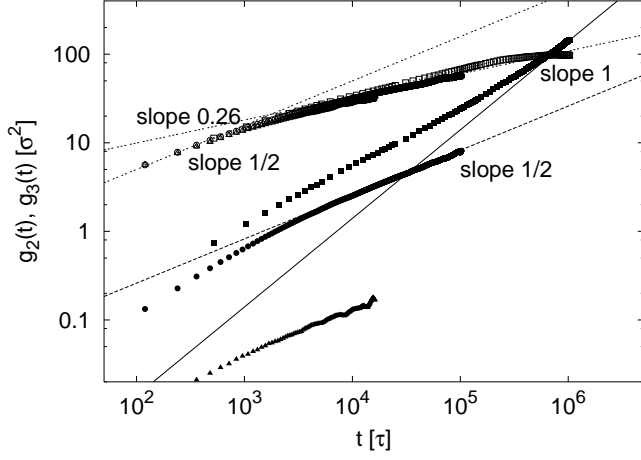


FIG. 1. Mean-square displacements  $g_2(t)$  (open symbols) and  $g_3(t)$  (closed symbols) for chain length  $N = 350$  ( $\square$ ),  $N = 700$  ( $\circ$ ) and  $N = 10000$  ( $\triangle$ ). The straight lines show some power law behaviors to guide the eye. The local reptation power laws  $g_2(t) \propto t^{1/4}$  and  $g_3(t) \propto t^{1/2}$  are verified with remarkable clarity.

$$g_1(t) = \begin{cases} 2b^2(Wt)^{\frac{1}{2}} & \text{for } t \lesssim \tau_e \\ \sqrt{\frac{2}{3}}bd_T(Wt)^{\frac{1}{4}} & \text{for } \tau_e \lesssim t \lesssim \tau_R \\ \sqrt{2}\frac{bd_T}{N^{\frac{1}{2}}}(Wt)^{\frac{1}{2}} & \text{for } \tau_R \lesssim t \lesssim \tau_d \\ 2\frac{d_T^2}{N^2}Wt & \text{for } \tau_d \lesssim t, \end{cases} \quad (4)$$

where  $W = \frac{k_B T}{\zeta b^2}$ ,  $d_T$  the effective tube diameter and  $\zeta$  is the effective bead friction.  $g_2(t)$  shows the same regimes for  $t < \tau_d$ , but goes to a plateau value of  $R_G^2(N)$  for  $t > \tau_d$ .

$$g_3(t) = \begin{cases} 6\frac{b^2}{N}Wt & \text{for } t \lesssim \tau_e \\ \frac{d_T^2}{N}(Wt)^{\frac{1}{2}} & \text{for } \tau_e \lesssim t \lesssim \tau_R \\ 2\frac{d_T^2}{N^2}Wt & \text{for } \tau_R \lesssim t, \end{cases} \quad (5)$$

where  $\tau_e$  is the entanglement time,  $\tau_R$  the Rouse time and  $\tau_d$  the disentanglement time [2]:

$$\tau_e = \frac{4}{9W} \left(\frac{d_T}{2b}\right)^4, \quad \tau_R = \frac{N^2}{3\pi^2 W}, \quad \tau_d = \frac{N^3}{\pi^2 W} \frac{b^2}{d_T^2}. \quad (6)$$

In Fig. 1 we show the results for  $g_2(t)$  for the innermost segments of the chains and  $g_3(t)$  for the systems with chain length  $N = 350, 700$  and  $10000$ . While the simulation times for  $N = 350$  were long enough to reach the diffusive regime the data for  $N = 700$  and  $10000$  just reach far into the predicted reptation regime.

After an initial Rouse-like motion  $g_2(t) \propto t^{1/2}$  for chains segments up to a time  $\tau_e = 1420 \pm 100\tau$  ( $N = 1100 \pm 100\tau$ ) for  $N = 700$  ( $N = 10000$ ) the motion slows down and is proportional to  $t^{0.26(1)}$  which is in remarkable agreement to the reptation model and is in less accordance with Schweizer's mode coupling theory [12]. The crossover time  $\tau_e$  leads us to our first estimate for  $N_e$  by assuming it to be the Rouse relaxation time of a subchain of length  $N_e$ . From the initial slope

of the short time Rouse-regime,  $g_1(t) = 0.525(5)\sigma^2(t/\tau)^{1/2}$ , we determine  $W = 0.025(2)\tau\sigma^{-2}$  which is consistent with a bead friction of  $\zeta = 25(1)\tau^{-1}$  determined separately by the relaxation of the Rouse modes of shorter chains [13]. Inserting this is into the expression for  $\tau_R$ , Eq. (6), yields  $N_e = 32(2)$  for  $N = 700$  and  $N_e = 28(2)$  for  $N = 10000$ . By equating the initial two power-law regimes for  $g_1(t)$  at  $\tau_e$ , we determine a tube diameter  $d_T = 7.6(3)$  for  $N = 700$ . Note, that for  $N = 10000$  the prefactor of the  $t^{0.26}$  regime appears about 7% smaller which gives  $d_T = 7.1(3)$ . Assuming that  $d_T = R^2(N_e)$  [2], where  $R^2$  is the end-to-end distance, gives  $N_e = 35(2)$  for  $N = 700$  and  $N_e = 32(2)$  for  $N = 10000$ . Thus the two ways of defining  $N_e$  give consistent results.  $d_T^2$  is also proportional to  $g_1(\tau_e)$ , though the exact prefactor is not strictly specified. Employing a Gaussian picture [7] of the tube one can estimate  $g_1(\tau_e) = 2R_G(N_e) = d_T^2/3$ . With the values of  $g_1(\tau_e, 700) = 18.9(5)$  and  $g_1(\tau_e, 10000) = 17.4(5)$  one obtains  $N_e = 35(1)$ ,  $d_T = 7.5(2)$  and  $N_e = 32(1)$ ,  $d_T = 7.2(2)$  respectively. These values agree with our old results [7] within error bars. After about the Rouse time  $\tau_R(N)$  the dynamics of  $g_2(t)$  should cross over to a second  $t^{1/2}$  regime, which corresponds to the diffusion of the whole chain along the gaussian tube contour. This second regime is not visible for  $N = 350$  since the chains are not long enough and only a broad crossover to the final plateau is observed. This regime should be more pronounced for  $N = 700$ , but the computational effort to obtain it is prohibitively large at present (about a CPU month on a 256 processor T3E). The slightly subdiffusive behavior of  $g_3(t)$  for times shorter than  $\tau_e$  is not due to entanglement effects and will be discussed elsewhere [13]. After  $\tau_e$  a clear  $t^{1/2}$  regime in  $g_3(t)$  is observed for  $N = 700$  and  $10000$ , in agreement with the reptation model rather than mode coupling [12]. The ratio of the power-law prefactors for these two chainlengths is  $18(2)$ . This is in good agreement again with the reptation model Eq. (5), where we expect a ratio  $16.3$  taking the slight  $N$ -dependence of  $d_T$  into account.  $g_2(t)$  for the shorter  $N = 350$  chains show a slightly higher exponent of  $t^{0.62(2)}$ . After about  $3.5 \cdot 10^5\tau$ , about twice the Rouse time  $\tau_R(350) = 1.8 \cdot 10^5\tau$ , the data show diffusive behavior.

Experimentally the motion of the segments can be obtained by measuring the time-dependent single-chain structure function

$$S(\mathbf{k}, t) = \frac{1}{N} \left\langle \sum_{i,j} \exp(i\mathbf{k} \cdot (\mathbf{r}_i(t) - \mathbf{r}_j(0))) \right\rangle. \quad (7)$$

For reptating chains this is predicted to be of the approximative form in the limits  $\frac{2\pi}{R_G} \lesssim k \lesssim \frac{2\pi}{d_T}$  and  $t > \tau_e$ :

$$\frac{S(k, t)}{S(k, 0)} = \left\{ [1 - \exp(-(kd/6)^2)] \cdot f\left(k^2 b^2 \sqrt{12Wt/\pi}\right) + \exp(-(kd/6)^2) \right\} \times \frac{8}{\pi^2} \sum_{p=1, \text{odd}}^{\infty} \frac{\exp(-tp^2/\tau_d)}{p^2}, \quad (8)$$

where  $f(u) = \exp(u^2/36)\text{erfc}(u/6)$ . The short time, Rouse-

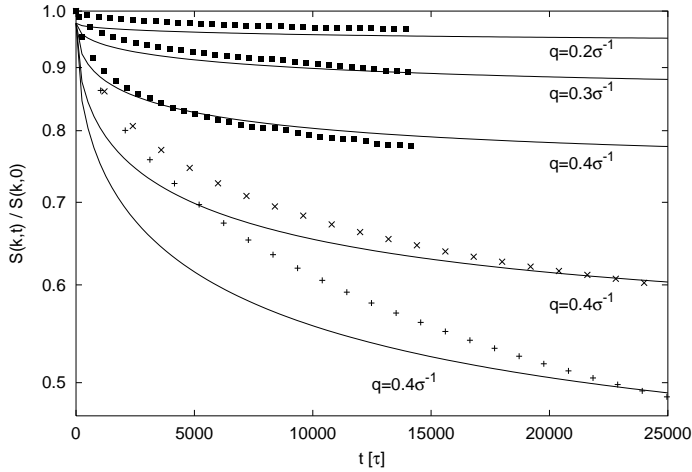


FIG. 2. Dynamic single chain structure function  $S(k, t)$  for different chain length  $N = 350$  (+),  $700$  ( $\times$ ), and  $10000$  ( $\blacksquare$ ) for various  $k$ -values. The solid lines are fits to Eq. (8) ( $d_T$  given in the text). For equal  $k$ -values the plateaus show a strong  $N$  dependence.

like motion is not described by this formula and only enters through the inverse friction coefficient  $W$ . The original formula was derived by de Gennes [14] on the basis of the reptation model and was slightly modified by Schlegel *et al.* [6] in an attempt to extend the range of validity of the original expression to larger  $k$ -vectors. Eq. (8) differs somewhat from the form given in ref. [6], as its time-dependence has been corrected due an argument by Kremer and Binder [15]. For the present set of data this correction is very small and can be neglected. Since for our system,  $d_T \simeq 7\sigma$ , the upper bound in  $k$ -space  $k_{max} \simeq 1.0\sigma^{-1}$ . The lower bound for each  $N$  with  $R_G = b^2N/6$  is  $k_{min}(N) \simeq 0.1(10000), 0.4(700), 0.8(350)\sigma^{-1}$ .

If one inserts  $\tau_d$ , Eq. (6), in Eq. (8) the resulting expression for  $S(k, t)$  contains only one adjustable parameter,  $d_T$ . We calculated  $S(k, t)$  for  $N = 350, 700$  and  $10000$  for several  $k$ -values between  $0.2 \leq k\sigma \leq 1.0$  and fitted the data to Eq. (8) in the time window  $5000\tau < t < 100000\tau$ . The best fit gives  $d_T = 15.7(5)\sigma$  for  $N = 350$  ( $k = 0.4\sigma^{-1}$ ),  $d_T = 12.7(3)\sigma$  for  $N = 700$  ( $k = 0.4\sigma^{-1}$ ) and  $d_T = 8.5(3)\sigma$  for  $N = 10000$  in a simultaneous fit to  $k = 0.2, 0.3$  and  $0.4\sigma^{-1}$ . Figure 2 shows our results together with the fitting curves. One can see that the agreement of Eq. (8) is only acceptable for  $N = 10000$  and  $N = 700$  and is rather poor for the shorter chains. The large difference between the tube diameter obtained from the data for different chain length suggests that finite chain length effects are much more important for  $S(k, t)$  than in  $g_1(t)$  in determining  $d_T$ . These finite chain length effects are not accounted for by Eq. (8). Clearly, the apparent value of  $d_T$  approaches our previous estimates of  $d_T$ , which should be expected since both methods measure the same quantity. For  $N = 10000$  finite chain length effects should be very small. Assuming a finite size scaling of  $d(N) = d_\infty + a/N^y$  a simple fit gives  $d_\infty = 7.65$  and  $y = 0.67$  showing that finite size

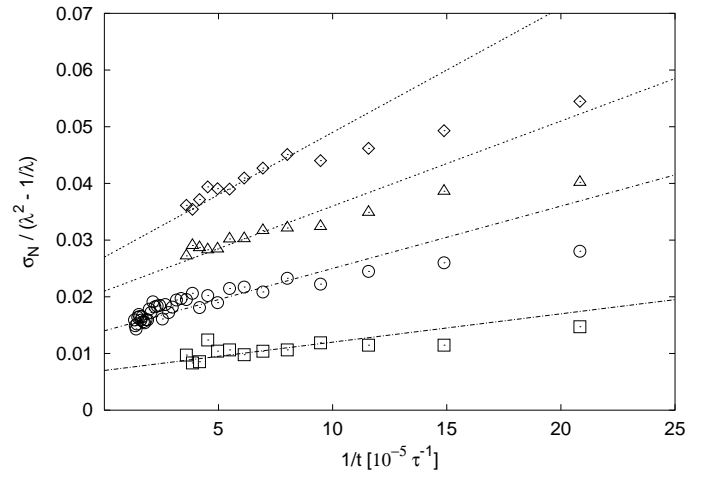


FIG. 3. Normal tension  $\sigma_N$  measured as a function of time after a step-strain for various strain amplitudes  $\lambda$  ( $1.25$  ( $\square$ ),  $1.5$  ( $\circ$ ),  $1.75$  ( $\triangle$ ) and  $2.0$  ( $\diamond$ )). The straight lines are fitted by hand to the long time decay of the stress to extrapolate the plateau stress.

effects decay very slowly and the extrapolated estimate for  $d_T$  agrees nicely with our estimate from  $g_1(\tau_e)$ .

The standard method to determine  $N_{e,p}$  (for clarity we index  $N_e$  determined from the plateau-modules with an additional index  $p$ ) experimentally is by measuring the plateau modulus in an oscillatory shear experiment. Alternatively, it is also possible to measure the normal stress decay in a step strain elongation. Since the latter is much simpler to perform in a simulation we ran volume conserving step strains for four different amplitudes  $\lambda = 1.25, 1.5, 1.75$  and  $2.0$ . After a rapid decay at short times, the stress had a well defined plateau from which we could determine  $G_N^0$  (see Fig. 3). The normal stress  $\sigma_N = \sigma_{xx} - (\sigma_{yy} + \sigma_{zz})/2$  was determined by the microscopic virial-tensor,  $x$  being the direction of elongation.

We fitted our results to the stress-strain formulas for classical rubber elasticity [16]  $\sigma_N = G(\lambda^2 - \frac{1}{\lambda})$  and to the Mooney-Rivlin (MR) formula [17]  $\sigma_N = 2G_1(\lambda^2 - \frac{1}{\lambda}) + 2G_2(\lambda - \frac{1}{\lambda^2})$  to determine  $G_N^0$ . The fit to the MR formula is excellent and gives  $G_N^0 = 0.0105k_B T\sigma^{-3}$  while the classical fit is fair and gives a value of  $G_N^0 = 0.008k_B T\sigma^{-3}$ . It is known experimentally that the MR formula slightly overestimates the modulus while the classical equation always underestimates it. The standard formula of Doi [2,18] to calculate  $N_{e,p}$ ,

$$G_N^0 = \frac{4}{5} \frac{\rho k_B T}{N_{e,p}}, \quad (9)$$

gives  $N_{e,p} = 65$  for the MR fit and  $N_{e,p} = 80$  for the classical formula. Both values are much higher than our previous estimate,  $N_e = 32$ .

If one scales the diffusion constant  $D(N)$  by the Rouse diffusion constant  $D_R(N)$  and plots it versus  $N/N_{e,p}$  experimental results for different polymers [19–21] and simulation results for different models [8,11] fall onto the same

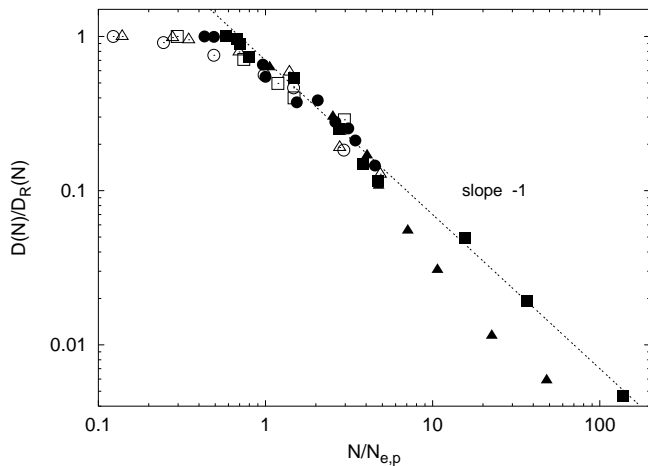


FIG. 4. Scaled diffusion constant  $D(N)/D_R(N)$  vs. scaled chain length  $N/N_{e,p}$  for polystyrene ( $\bullet$ ) [21] ( $M_{e,p} = 14600$ ,  $T = 485K$ ), polyethylene ( $\blacksquare$ ) [19] ( $M_{e,p} = 870$ ,  $T = 448K$ ), PEB2 ( $\blacktriangle$ ) [20] ( $M_{e,p} = 992$ ,  $T = 448K$ ), our bead spring model ( $\triangle$ ) ( $N_{e,p} = 72$ ), the bond-fluctuation model for  $\Phi = 0.5$  ( $\square$ ) [8] and tangent hard spheres at  $\Phi = 0.45$  ( $\circ$ ) [11]. All data are scaled with  $N_{e,p}$  from the plateau modulus or with  $2.2N_e$  from  $g_1(t)$ .

universal curve (see Fig. 4 [22]). The diffusion constants for the simulated systems are determined by extrapolating  $g_3(t \rightarrow \infty)$ . Using a value  $N_{e,p} = 72$ , intermediate between the MR and classical fits to the stress-strain data, to normalize  $N$ , our results nicely fall onto the experimental values. For the bond-fluctuation [8] and tangent hard sphere models [11] no plateau-moduli are available, thus we scaled  $N_e$  calculated from  $g_1(\tau_e)$  in these models (bond-fluctuation:  $N_e = 30$ , tangent hard sphere:  $N_e = 29$ ) by the same factor of  $N_{e,p}/N_e = 72/32 = 2.25$  obtained from our model to estimate  $N_{e,p}$ . However, due to the uncertainty and limited range of the simulation data and the scatter in the experimental data,  $N_{e,p}$  in the range  $2.0 - 2.4N_e$  could also be chosen to collapse the data. The nice collapse of the data supports our assumption that  $N_e$  and  $N_{e,p}$  are related by a universal multiplicative factor of about 2.2. It remains unclear though whether this prefactor of about 2.2 is truly universal or just a consequence of the fact that all three model systems are fully flexible and have almost the same packing fractions.

In the light of our simulation results one should critically review the results of recent NSE experiments [6] which claim to support the reptation prediction and rule out other theories by fitting the data to Eq. (8). They also claim that their estimated value of  $N_e$  agrees nicely with the value derived from the plateau modulus. However, it should be noted that the chain lengths in these investigations are only about twice our  $N = 700$  chains, i.e.  $N \approx 23N_{e,p}$ , in a comparable range of  $k$ -vectors. The simulation results suggest, that  $d_T$  determined in these experiments is systematically too high by about a factor of 1.5, giving a factor of 2 for  $N_e$ . Note, that the finite chain length effects are much stronger in  $S(k, t)$  than in  $g_2(t)$ .

To conclude, we find that our data are in very good agree-

ment to the predictions of the reptation model. The dynamical exponent of  $t^{1/4}$  for the local reptation regime has been verified with remarkable clarity. We further demonstrate that very long chains with  $N > 100N_{e,p}$  are needed for  $S(k, t)$  to arrive at a consistent prediction of  $N_e$  with that from the mean-square displacements. The most recent experiments were performed for chain lengths well below this threshold. In contrast the formula for the modulus by Doi leads to an estimate of  $N_e$  larger by a factor of about 2.2(2). Whether this discrepancy is due to just uncertainties in prefactors of the reptation model or due to the failure of the classical single chain picture for the viscoelasticity still remains unclear.

Most of the simulations were carried out at the Rechenzentrum of the MPG in Munich and at Exxon Research and Engineering Company. Sandia is a multiprogram laboratory operated by Sandia Corporation, a Lockheed Martin Company, for the United States Department of Energy under Contract DE-AC04-94AL85000.

- 
- [1] P. G. de Gennes, *Scaling Concepts in Polymer Physics* (Cornell University Press, Ithaca, 1979).
  - [2] M. Doi and S. F. Edwards, *The Theory of Polymer Dynamics* (Clarendon Press, Oxford, 1986).
  - [3] P. R. Rouse, *J. Chem. Phys.* **21**, 1272 (1953).
  - [4] R. Kimmich and H. W. Weber, *J. Chem. Phys.* **98**, 5847 (1993).
  - [5] B. Ewen and D. Richter, *Adv. Polym. Sci.* **134**, 3 (1997).
  - [6] P. Schleger *et al.*, *Phys. Rev. Lett.* **81**, 124 (1998).
  - [7] K. Kremer and G. S. Grest, *J. Chem. Phys.* **92**, 5057 (1990).
  - [8] W. Paul, K. Binder, D. W. Heermann, and K. Kremer, *J. Chem. Phys.* **95**, 7726 (1991).
  - [9] B. Dünweg, G. S. Grest, and K. Kremer, in *Numerical Methods for Polymeric Systems*, edited by S. G. Whittington (Springer, Berlin, 1998), Vol. IMA Vol. 102, p. 159.
  - [10] J. Skolnick and A. Kolinski, in *Advances in Chem. Phys.*, edited by I. Prigogine and S. A. Rice (Wiley, New York, 1990), p. 223.
  - [11] S. W. Smith, C. K. Hall, and B. D. Freeman, *J. Chem. Phys.* **104**, 5616 (1996).
  - [12] K. S. Schweizer, *J. Chem. Phys.* **91**, 5822 (1989).
  - [13] M. Pütz and K. Kremer, to be published.
  - [14] P. G. de Gennes, *J. de Phys.* **42**, 735 (1981).
  - [15] K. Kremer and K. Binder, *J. Chem. Phys.* **81**, 6381 (1984).
  - [16] L. R. G. Treloar, *The Physics of Rubber Elasticity* (Clarendon Press, Oxford, 1986).
  - [17] M. Mooney, *J. Appl. Phys.* **11**, 582 (1940).
  - [18] M. Doi, *J. Polym. Sci.* **18**, 1005 (1980).
  - [19] D. S. Pearson, G. V. Strate, E. von Merwall, and F. C. Schilling, *Macromolecules* **20**, 1133 (1987), the value of  $M_{e,p} = 830$  ( $T = 413K$ ) taken from [23] was corrected for temperature using their packing model. This gives  $M_{e,p} = 870$  at  $T = 448K$ .
  - [20] D. S. Pearson *et al.*, *Macromolecules* **27**, 711 (1994), the quoted value of  $M_{e,p} = 1240$  in this work did not take the prefactor  $4/5$  of Eq. (9) into account. To be consistent with our definitions, we used  $4/5 \cdot 1240 = 992$ .

- [21] M. Antonietti, K. J. Fölsch, and H. Sillescu, *Macromolekulare Chemie* **188**, 2317 (1987), the value  $M_{e,p} = 14600$  was taken from [23] and corrected for the difference in temperature following the packing model described in [23].
- [22] The experimental data are corrected for the temperature difference to the glass transition temperature  $T_G$ , but for simulation data the correction is negligible. In earlier publications [7,9] the scaling of  $D$  versus  $N/N_e$  was done with  $N_e$  determined from  $g_1(t)$  for simulation data since plateau-moduli were not available at that time. Further, experimental data were not corrected for the proximity of the glass transition. This led to an underestimation of  $N_{e,p}$  for the simulation models.
- [23] L. J. Fetters *et al.*, *Macromolecules* **17**, 4639 (1994).